Experimental Microwave Validation of Level Set Reconstruction Algorithm

Douglas A. Woten, Mohammad R. Hajihashemi, Ahmed M. Hassan, and Magda El-Shenawee

***Abstract*—The capability of the level set method is illustrated for shape and location reconstruction using real measurement data in the range of 3–8 GHz. An experimental setup is utilized to measure the S-parameters using two Vivaldi antennas revolving around metallic pipes of different cross-sections. A two-dimensional reconstruction of the pipe's cross section is retrieved using the level set algorithm combined with the Method of Moments and the frequency hopping technique. The results show good agreement between the reconstructed cross section and the true configuration. This indicates to the strength of the level set method and its ability to cope with the noise in real measurements.**

***Index Terms*—Image reconstruction, inverse problem, level set algorithm, measured microwave data.**

I. Introduction

The level set algorithm has been demonstrated to be versatile in reconstructing the shape and location of irregular shaped objects of various compositions [1]–[9]. Papers [3] and [9] consider perfect electric conductors (PEC) while [4], [7], and [8] are used with dielectric materials. The majority of published results using the level set method are based on synthetic data with varying amounts of artificial noise injected into the signal. In 2000 the Institut Fresnel started a public repository of scattered microwave data that has been used for validating inversion techniques [5]–[8], [10]. The microwave measurements system at the Institut Fresnel consisted of a spherical scanning system housed in an anechoic chamber 14.2 m in length and 6.5 m in width and height respectively. The transmitting and receiving antennas were wide band horn antennas. That system was designed to operate in a frequency between 300 MHz to 26.5 GHz with angular accuracy within 0.05° [5], [6].

Ramananjaona *et al.* have used the Institut Fresnel experimental data for the reconstruction of metallic pipes and presented reconstruction results for the *TE* and *TM* data on circular, rectangular and U-shaped pipes [7]. Litman employed the Institut Fresnel data for the reconstruction of dielectric objects that are homogeneous by parts and of known characteristics [8].

The purpose of the current work is to augment the experimental works described above with a different microwave measurements system. The details pertaining to the version of the level set algorithm used in this work is described in [9]. The existing system uses two Vivaldi antennas rotating around the target as will be described in Section II [11]. In this work circular, square and hexagonal metallic pipes are utilized to approximate PEC objects and the results are reported in Section V.

Manuscript received October 23, 2008; revised May 14, 2009. First published November 06, 2009; current version published January 04, 2010. This work was supported in part by Entergy Arkansas Inc., NSF Graduate Research Fellowship, NSF GK-12 Program, NSF Award Number ECS–0524042, and in part by the Arkansas Biosciences Institute (ABI).

D. A. Woten is with the Microelectronics-Photonics Program (MicroEP), University of Arkansas, Fayetteville, AR 72701 USA (e-mail: dwoten@uark.edu)

R. Hajihashimi, A. M. Hassan, and M. El-Shenawee are with the Electrical Engineering Department, University of Arkansas, Fayetteville, AR 72701 USA (e-mail: mhajihas, amhassan, magda@uark.edu)

Color versions of one or more of the figures in this communication are available online at http://ieeexplore.ieee.org.

Digital Object Identifier 10.1109/TAP.2009.2036186

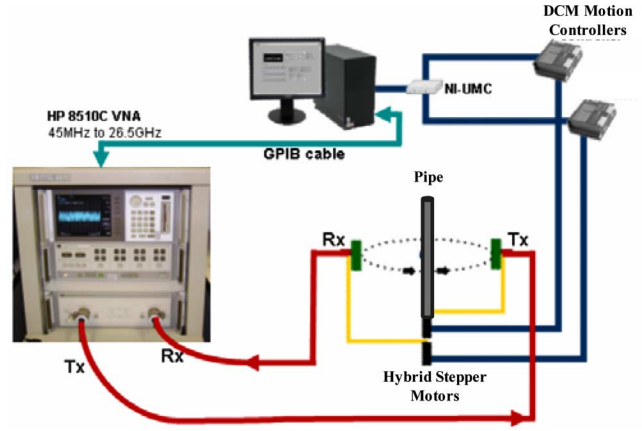

Fig. 1. Schematic of experimental setup.

II. Experimental Setup

The experimental setup relies on a HP 8510C Vector Network Analyzer (VNA). This 2-port VNA model allows for frequency sweeps between 45 MHz to 26.5 GHz with up to 801 points per sweep. The VNA communicates directly with a central computer through a GPIB cable. The computer provides a central control for all the various components and acts as a collection point for the generated data. An antenna is connected to each port of the VNA to allow for the measurement of the four S-parameters (S_{11}, S_{12}, S_{21}, and S_{22}). Each of these antennas (T_x, R_x) is connected to rotating arms controlled by independent HIS DCM 8028 motion control drivers. The drivers receive input from the National Instruments Universal Motion Controller (UMC) and each control a PowerMax II hybrid stepper motor. This allows each antenna to rotate around a central location independently. A schematic of the experimental setup is shown in Fig. 1.

The transmitter, T_x, and receiver, R_x, employed in this work are Vivaldi antennas [12]. Any linearly polarized broadband antenna could be used; however, the Vivaldi antennas were readily available in the laboratory and operate between 3–8 GHz. A schematic of the Vivaldi antenna along with the material parameters is shown in Fig. 2(a). Fig. 2(b) shows the S_{11} of each antenna. The performance of Antenna #2 is deteriorated at frequencies above 8 GHz possibly due to a mismatch between the antenna and SMA connector (not shown here). Fig. 2(c) shows the S_{21} and S_{12} of the antennas.

The Vivaldi antenna has a focused antenna beam as shown in Fig. 3. The commercial software package Ansoft High Frequency Structure Simulator (HFSS) is used to simulate the Vivaldi antenna of Fig. 2. The resulting antenna pattern in the E and H-planes are shown in Fig. 3(a) and (b) respectively. The results of Fig. 3 show the Vivaldi beamwidth is approximately 80° in the H -plane and 35° in the E-plane. The direction of the main beam shifts from 125° at 3 GHz to 97° at 8 GHz. Note that the metallizations on the front and back of the antenna substrate are not symmetric as shown in Fig. 2(a).

To reduce interference from the surroundings, an anechoic chamber is built to house the rotating antennas and the pipe as shown in Fig. 4. The chamber is a one meter cube with EHP-5PCL microwave pyramidal absorber. This absorber has a maximum reflection of -30 db at

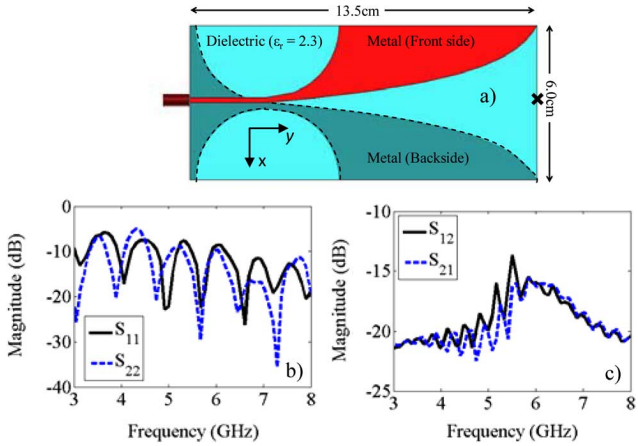

Fig. 2. (a) Geometry of Vivaldi antenna, (b) measured S_{11} and S_{22} and (c) measured S_{12} and S_{21}.

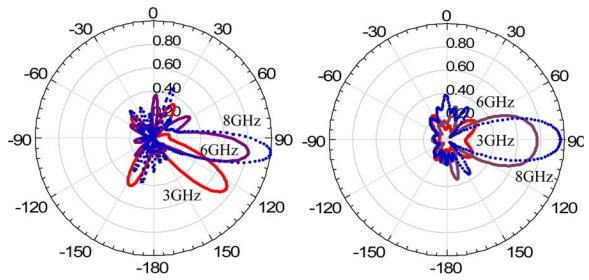

Fig. 3. The radiation pattern of the Vivaldi antennas in the (a) E-Plane and (b) H-Plane.

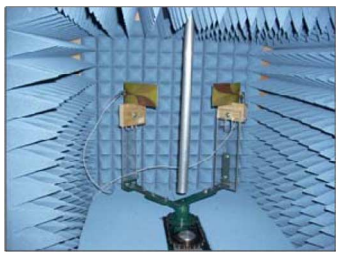

Fig. 4. Anechoic chamber of 1 m^3 with two Vivaldi antennas rotating around a pipe.

frequencies above 2 GHz and is approximately 12.5 cm thick. As a result, the useable space inside the chamber is approximately 75 cm^3.

III. Complex Antenna Factor

Inversion algorithms use the complex electric fields as the input [1]–[10] while the VNA measures the complex scattering parameters. To validate the level set algorithm the S-parameters are first converted to electric fields using a *transfer function* similar to that in [13]. In this work, the transfer function represents the ratio of electric field, E_x, to the S-parameter, S_{21}. The E_x represents the complex electric field in the x-direction at the front end of the receiving antenna and S_{21} represents the complex measurement at antenna 2 when antenna 1 is excited. These quantities are both obtained when no target is present in the experimental set-up [11], [13]. The transfer function is a complex number, antenna dependent, referred to as the *complex antenna factor (CAF)* and given by $\mathrm{CAF} = E_{\mathrm{x}}/S_{21}$. The commercial electromagnetic simulator, FEKO, is used to simulate E_{x} and S_{21} to

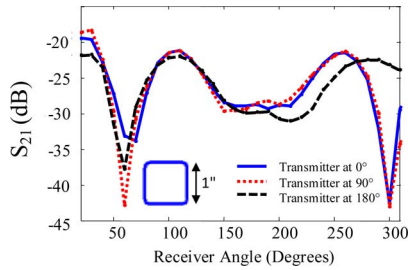

Fig. 5. The measured S_{21} at each receiver angle for 3 GHz.

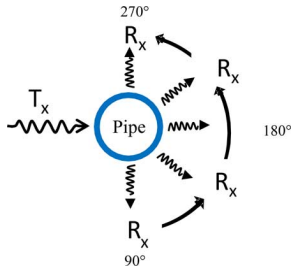

Fig. 6. An example of the data collection for a single transmitting location.

calculate the CAF at all frequencies and all incident and receiving angles. The FEKO package provides faster electric field calculations of large geometries when compared with the HFSS.

A sample of the S_{21} measured data from the square pipe is shown in Fig. 5 which illustrates the variations of the S_{21} with the receiver angles at 3 GHz. Fig. 5 has three curves corresponding to three different transmitter angles (0°, 90° and 180°) where the receiver angle is always measured with respect to the transmitter angle. Theoretically, the three plots should be identical; however, discrepancies are observed around the receiving angle of 300°. This could be attributed to the coupling between the two antennas since they are closest to each other at this angle (see Fig. 6).

IV. Reconstruction Results

A. Level Set Algorithm

In this work the configuration of the pipe immersed in air is considered two-dimensional (2D) since the length of the pipe is much larger than the wavelength with uniform cross-section. The 2D perfect electric conductor (PEC) level set algorithm of [9] is used to reconstruct the shape and location of the pipe with three different cross sections. The level set algorithm assumes that the interface is represented implicitly as the zero level of a higher order function ϕ. At each time t, the interface is defined as [3]:

$$\Gamma(t) = \{(x, y) | \phi(x, y, t) = 0\} \tag{1}$$

Once the derivative with respect to time is found, the Hamilton-Jacobi equation for tracking the motion of the interface is obtained [3], [4]

$$\frac{\partial \phi}{\partial t} + F\|\nabla \phi\| = 0 \tag{2a}$$

$$\phi_0 = \phi(x, y, t = 0) \tag{2b}$$

where F is the normal component of the deformation velocity. The Method of Moments is used as the forward solver and the frequency hopping technique is used from 3–8 GHz (the antenna range) in steps

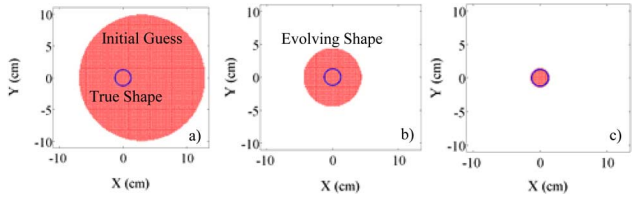

Fig. 7. Reconstruction of circular pipe (a) initial guess at 3 GHz, (b) after 2505 iterations at 3.5 GHz, and (c) after 5025 iterations at 5 GHz.

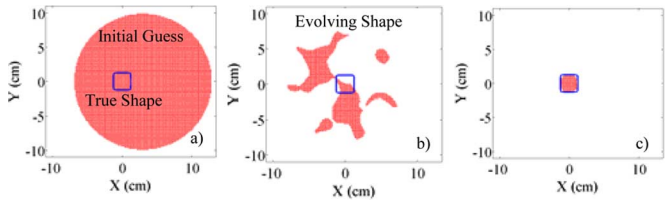

Fig. 8. Reconstruction of square pipe with rounded corners (a) initial guess at 3 GHz, (b) after 4005 iterations at 4.5 GHz ,and (c) after 8490 iterations at 6.8 GHz.

that range from 200–500 MHz. Additional details of this specific level set algorithm are reported in [9].

B. Measurement Configuration

The front of the two antennas, marked x in Fig. 2(a), is set at a distance of 7.8 cm from the center of the chamber where the pipe is positioned. Antenna #1 is fixed at directions from 0°–360° in steps of 10° while Antenna #2 collects data at directions 90°–270° with respect to antenna #1 in steps of 10°. Fig. 6 shows the data collection scheme. The symmetry of the pipes in this work allows using less data in the algorithm as will be discussed in each case. In all results the initial guess is a circle of diameter 20 cm centered at (3, 0).

C. Case 1 (Circular Pipe)

The first case considered in this work is a pipe with a circular cross-section. The pipe is $1''$ in diameter (2.54 cm) and is made of aluminum. For this work the pipe is approximated as a PEC. The image reconstruction is shown in Fig. 7(a)–(c). After 2505 iterations, Fig. 7(b) shows the evolving shape which remains circular. In the 5025th iteration, Fig. 7(c) shows the reconstructed shape that converges to the true configuration.

D. Case 2 (Square Pipe)

The square pipe is the second case considered in this work. The pipe has slightly rounded corners, is $1''$ in length on each side (2.54 cm), made of steel and is approximated as a PEC for this work. Due to symmetry of the pipe, the data measured for the transmitting angle 0°–90° is repeated for the input to the level set algorithm. The reconstruction is shown in Fig. 8(a)–(c). After 4005 iterations the evolving shape has split into multiple ones seemingly unrelated to the true shape as shown in Fig. 8(b). The reconstruction achieves good agreement with the true object after 8490 iterations as shown in Fig. 8(c). The reconstructed shape is slightly smaller especially at the corners as shown in Fig. 8(c).

E. Case 3 (Hexagonal Pipe)

The final case considered in this work is the hexagonal pipe. The pipe is $1''$ in diameter (2.54 cm), made of aluminum and approximated as a PEC object similar to Case 1. Due to symmetry the data measured for the transmitting angle 0°–60° is repeated for the input to the level set algorithm. The reconstruction is shown in Fig. 9(a)–(c). The reconstruction is shown after 1600 iterations in Fig. 9(b). The final reconstruction has good agreement with the true shape after 20100 iterations as shown in Fig. 9(c).

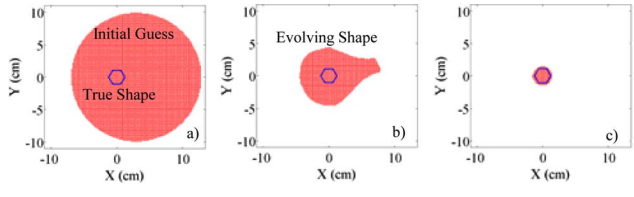

Fig. 9. Reconstruction of hexagonal pipe (a) initial guess at 3 GHz, (b) after 1600 iterations at 3.25 GHz, and (c) after 20100 iterations at 8 GHz.

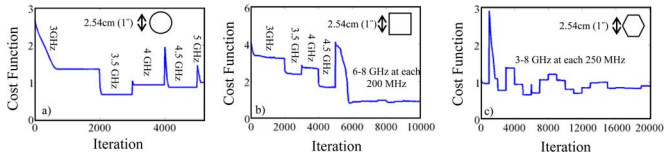

Fig. 10. Cost function for the (a) circular pipe, (b) square pipe, and (c) hexagonal pipe.

The cost function, which is normalized with respect to the measurement data, gives the error between the simulated evolving shape and the measured data, is shown in Fig. 10(a)–(c). Note that the frequency hopping causes the cost function to display stair-like and/or jumping behavior as the frequency is hopped to the following frequency [3], [9]. More frequencies are used for the hexagonal reconstruction (20 frequencies in steps of 250 MHz) vs. the square (15 frequencies in steps of 500 MHz then 200 MHz) and the circle (5 frequencies in steps of 500 MHz). The need for more frequencies is due to the presence of six corners in the hexagonal vs. four corners in the square and no corners in the circular cases. It is known that higher frequencies are needed to retrieve the fine details of the target's shape.

V. Conclusion

In this work measurement data from our experimental system is utilized to validate the level set algorithm for 2D PEC shapes. When considering the error in the cross-section area of the reconstructed shapes, it is observed to be on the order of 5% or less for the cases examined here. The effect of variations in the number of measurement points and antenna distances is discussed in [9].

The reconstruction requires approximately 4–7 CPU hours, depending on the geometry, on a single 64-bit AMD Opteron 246 processor running at 2 GHz. Additional higher frequencies are needed to reconstruct the fine details of complex shapes and thus increase the computational time requirements. Current work in parallelizing the code for the level set algorithm has resulted in a speedup of 100X employing 256 processors on the San Diego Supercomputer Center's DataStar [14]. This speedup allows for reconstruction results in 2.5–4.5 minutes compared to 4–7 hours. Ongoing research by the authors considers 3D objects [15].

Acknowledgment

The authors would like to thank Mr. Kegege for his help in this work.

References

[1] J. A. Sethian, *Level Set Methods and Fast Marching Methods*. Cambridge, U.K.: Cambridge Univ. Press, 1999.

[2] S. J. Osher and R. P. Fedkiw, *Level Set Methods and Dynamic Implicit Surfaces*. New York: Springer-Verlag, 2003.
[3] R. Ferraye, J. Y. Dauvignac, and C. Pichot, "An inverse scattering method based on contour deformations by means of a level set method using frequency hopping technique," *IEEE Trans. Antennas Propag.*, vol. 51, no. 5, pp. 1100–1113, May 2003.
[4] O. Dorn and D. Lessselier, "Level set methods for inverse scattering," *Inverse Problems*, vol. 22, no. 4, pp. R67–R131, Aug. 2006.
[5] K. Belkebir, S. Bonnard, F. Pezin, P. Sabouroux, and M. Saillard, "Validation of 2D inverse scattering algorithms from multi-frequency experimental data," *J. Electromagn. Waves Applicat.*, vol. 14, pp. 1637–1667, 2000.
[6] J. Geffrin, P. Sabouroux, and C. Eyraud, "Free space experimental scattering database continuation: experimental set-up and measurement precision," *Inverse Problems*, vol. 25, no. 6, pp. S117–S130, Dec. 2005.
[7] C. Ramananjaona, M. Lambert, and D. Lesselier, "Shape inversion from TM and TE real data by controlled evolution of level sets," *Inverse Problems*, vol. 17, no. 6, pp. 1585–1595, Dec. 2001.
[8] A. Litman, "Reconstruction by level sets of n-ary scattering obstacles," *Inverse Problems*, vol. 21, no. 6, pp. S131–S152, Dec. 2005.
[9] M. R. Hajihashemi and M. El-Shenawee, "Using the level set method for microwave applications," *IEEE Antennas Wireless Propag. Lett.*, vol. 7, pp. 92–96, 2008.
[10] C. Gilmore, P. Mojabi, and J. LoVetri, "Comparison of the distorted born iterative and multiplicative-regularized contrast source inversion methods: The 2D TM case," in *Proc. Annu. Rev. of Progress in Appl. Comput. Electromagn.*, Niagara Falls, Canada, Mar. 30–Apr. 4 2008, pp. 122–127.
[11] D. A. Woten, O. Kegege, R. Hajihashimi, A. Hassan, and M. El-Shenawee, "Microwave detection using real measurement data," in *Proc. Annu. Rev. of Progress in Appl. Comput. Electromagn.*, Niagara Falls, Canada, Mar. 30–Apr. 4 2008, pp. 650–655.
[12] O. Kegege, "Ultra-Wide Band Radar for Near-Surface and Buried Target Detection," M.S. thesis, Univ. Texas Pan American, Edinburg, TX, 2006.
[13] S. Ishigami, H. Iida, and T. Iwasaki, "Measurements of complex antenna factor by the near-field 3-antenna method," *IEEE Trans. Electromag. Compat.*, vol. 38, no. 3, pp. 424–432, Aug. 1996.
[14] M. R. Hajihashemi and M. El-Shenawee, "MPI parallelization of the level-set reconstruction algorithm," presented at the IEEE Int. Symp. on Antennas Propag./URSI Nat. Radio Science Meeting, Charleston, SC, Jun. 1–5, 2009.
[15] M. R. Hajihashemi and M. El-Shenawee, "Three-dimensional level set algorithm for shape reconstruction of conducting objects," presented at the IEEE Int. Symp. on Antennas Propag./URSI Nat. Radio Science Meeting, Charleston, SC, Jun. 1–5, 2009.

Scattering of Electromagnetic Waves From a Rectangular Plate Using an Enhanced Stationary Phase Method Approximation

Charalampos G. Moschovitis, Konstantinos T. Karakatselos, Efstratios G. Papkelis, Hristos T. Anastassiu, Iakovos Ch. Ouranos, Andreas Tzoulis, and Panayiotis V. Frangos

***Abstract*—A time-efficient high frequency analytical model for the calculation of the scattered field from a perfect electric conductor (PEC) plate is presented here, which is based on the physical optics (PO) approximation and the stationary phase method (SPM). Using the SPM analysis for the three-dimensional (3D) scattering problem under consideration, the scattered electric field is calculated analytically. It follows that the analytical formula proposed here yields an accurate and fast algorithm for the calculation of the scattered electromagnetic (EM) field, which can be used trustfully in a variety of radio propagation problems. The accuracy of the proposed analytical method is checked through a straightforward numerical integration over the PO currents, as well as through Finite Element Boundary Integral full-wave exact solution. Comparison results are given in the far field, Fresnel zone and the near field area.**

***Index Terms*—Physical optics approximation, radio coverage, scattered field calculation, stationary phase method.**

I. Introduction

Considering radio propagation in urban outdoor areas [1], analytical EM methods for scattering and diffraction from building walls may be preferable to empirical models or actual radio propagation experiments. For such problems analytical EM methods are usually found to be more accurate than empirical methods, even though in most cases they are slower in terms of actual calculation time.

In this communication we analyze the implementation of an analytical model based on an enhanced version of the stationary phase method (SPM) approximation for the calculation of the vector potential $\underline{A}$, and subsequently of the electric field $\underline{E}$, in a three-dimensional (3D) scattering electromagnetic problem. The proposed method derives from the extension of the corresponding problem in two dimensions to the three-dimensional scattering problem examined here. It is found that the proposed 3D analytical method is much faster than the standard approach [1], which employs numerical integration over the PO currents.

Our proposed method can be incorporated, for example, to simulation tools that produce radiocoverage patterns in urban outdoor environments, in which first or higher order scattering mechanisms are considered [1]. Assuming that the PEC plate simulates a wall-scatterer (for which an appropriate reflection coefficient has to be included, in

Manuscript received February 12, 2008; revised April 16, 2009. First published May 27, 2009; current version published January 04, 2010.

C. G. Moschovitis, K. T. Karakatselos, E. G. Papkelis, I. C. Ouranos, and P. V. Frangos are with the School of Electrical and Computer Engineering, Division of Information Transmission Systems and Materials Technology, National Technical University of Athens, GR-15780 Zografou, Athens, Greece (e-mail: pfrangos@central.ntua.gr; harism@noc.ntua.gr).

H. T Anastassiu is with the Hellenic Aerospace Industry, GR-32009 Schimatari-Tanagra/Viotia, Greece.

A. Tzoulis was with the Department of Antennas and Scattering (AuS), Research Establishment for Applied Science (FGAN), Research Institute for High Frequency Physics and Radar Techniques (FHR), D-53343 Wachtberg, Germany. He is now with the New Technologies and Applications Group (NTAG) of TELETEL S.A., GR-11526 Athens, Greece.

Color versions of one or more of the figures in this communication are available online at http://ieeexplore.ieee.org.

Digital Object Identifier 10.1109/TAP.2009.2024015